European Journal of Medicinal Chemistry 143 (2018) 1174–1184

Contents lists available at ScienceDirect

European Journal of Medicinal Chemistry

journal homepage: http://www.elsevier.com/locate/ejmech

Research paper

A routinely used protein staining dye acts as an inhibitor of wild type and mutant alpha-synuclein aggregation and modulator of neurotoxicity

Nuzhat Ahsan [a], Ibrar Ahmed Siddique [a], Sarika Gupta [a, **], Avadhesha Surolia [b, *]

[a] Molecular Science Lab, National Institute of Immunology, New Delhi 110067, India
[b] Molecular Biophysics Unit, Indian Institute of Science, Bangalore 560012, India

ARTICLE INFO

Article history:
Received 29 August 2015
Received in revised form
27 September 2017
Accepted 2 October 2017
Available online 12 October 2017

Keywords:
α-Synuclein
Triphenylmethane dyes
Aggregation
Fibrillisation
A11
Synucleinopathies
Parkinson's disease

ABSTRACT

Inhibition of amyloid formation along with modulation of toxicity employing small molecules is emerging as a potential therapeutic approach for protein misfolding disorders which includes Parkinson's disease, Alzheimer's disease and Multiple System Atrophy etc. Countless current interventional strategies for treating α-synucleinopathies consider using peptidic and non-peptidic inhibitors for arresting fibrillisation, disrupting existing fibrils and reducing associated toxicity. One group of molecules less exploited in this regard are triphenylmethane dyes. Herein we tested the inhibitory effect of two routinely used protein staining dyes *viz* Coomassie Brilliant blue G (CBBG) and Coomassie Brilliant blue R (CBBR) employing several biophysical and cell based methods. Our results showed that both the dyes not only efficiently inhibit fibrillisation but also disrupt existing fibrils. Nonetheless, only CBBR prevented the appearance of A11 epitopes which are marker of toxicity. Moreover, CBBR was also able to stall fibrillisation of A53T mutant α-synuclein and reduce associated neurotoxicity. This study thus reports the potential of CBBR as a therapeutic molecule.

© 2017 Elsevier Masson SAS. All rights reserved.

1. Introduction

Several lines of evidence suggest that self association of protein monomers into amyloids destabilises the native soluble and harmless form of a protein and converts it essentially into cross β structure rich stable, insoluble filamentous aggregates [1–4]. Protein aggregation and neurodegeneration in the brain has been a subject of intense scientific scrutiny. Though several proteins are expressed ubiquitously, they specifically affect the nervous system when aberrantly misfolded and aggregated. Among quite a lot of neurodegenerative diseases with variety of proteins involved, the term "Synucleinopathies" is assigned to a subset of disorders comprising common pathological hallmark *viz.* 'aggregation of α-synuclein' in specific neuronal and glial populations. Examples of synucleinopathies include Parkinson's disease (PD), Dementia with Lewy bodies (DLB), and Multiple system atrophy (MSA). Besides having α-synuclein as a common pathological characteristic, all these diseases are clinically distinguished by a progressive decrease in cognitive, motor, behavioural and autonomic function [5].

α-synuclein is considered a natively unfolded pre-synaptic protein monomer composed of 140 amino acids with molecular weight 14.46 kDa [6]. It is found both in cytosol and in association with membranes. Its physiologic form appears to be a tetramer [7–11]. Though the exact role of α-synuclein is still a matter of study, there are clear indications of its importance in several vital physiological processes. The normal physiological functions of α-synuclein have been proposed based on its structure, physical properties and interacting partners [12]. Its ubiquitous presence in body and intrinsically disordered nature facilitates binding to multiple proteins and ligands and performing different functions [13]. However, genetic multiplication, mutations (A30P, E46K and A53T) and environmental stress can cause the protein to misfold and aggregate into non-amyloid amorphous aggregates or highly ordered amyloid fibrils [14].

As the link between α-synuclein aggregation and neurodegeneration has been in prevalence for a long time not only for PD and other synucleinopathies but also for other debilitating disorders, there is a growing interest to search molecules that can reduce

* Corresponding author.
** Corresponding author.
E-mail addresses: sarika@nii.ac.in (S. Gupta), surolia@mbu.iisc.ernet.in (A. Surolia).

https://doi.org/10.1016/j.ejmech.2017.10.002
0223-5234/© 2017 Elsevier Masson SAS. All rights reserved.

Abbreviations

PD	Parkinson's disease
CBBG	Coomassie Brilliant Blue G
CBBR	Coomassie Brilliant Blue R
WtAS	Wild Type Alpha-Synuclein
ThT	Thioflavin T
BBB	Blood Brain Barrier

the production of α-synuclein, promote clearance of accumulated synuclein and increase the stability of native form so as to prevent misfolding [15].

Though the list of anti-amyloid molecules for treating synucleinopathies is on the rise, the search is still on. Among the major categories of aggregation inhibitors which include proteins/peptides and nanoparticles, the most attractive option is discovering or designing novel small molecule inhibitors. Years of research have thus yielded three main categories of inhibitors [16]: (*i*) Proteins and peptides such as molecular chaperones, antibodies and β-sheet breakers [17,18]; (*ii*) Nanoparticles [19,20] and (*iii*) Small molecules such as polyphenols, metal chelators etc. [21–23].

The therapeutic action of all the proposed classes of inhibitors has its own set of pros and cons. The biggest challenge for proteins and peptide-based inhibitors is their vulnerability to degradation by proteases and mounting of immune responses among others such as their inefficacy in crossing the blood brain barrier. Additionally, peptidic and nanoparticle based strategies are even expensive and labour intensive.

In comparison to other classes, small molecule inhibitors are cost effective and easier to deal with. This class faces the challenges of specificity and can have multiple targets inside a cellular system which needs to be understood and taken care of while using new naturally occurring small molecules or embarking on *de novo* synthesis.

In search of therapeutic agents that specifically and efficiently inhibit aggregation process, several groups of compounds have been reported which either inhibit oligomerisation (Class I compounds) or fibrillisation (Class III compounds) or both oligomerisation and fibrillisation (Class II compounds) [24]. These compounds include polyphenols such as curcumin and their derivatives, dyes such as ThT, indomethacin, Congo red, Phenol red, Eosin Y etc [21,25,26].

It is a well established that inhibition of oligomerisation or fibrillisation or both though sought after, is of limited value without modulation of their toxicity. Currently neurotoxicity is attributed to soluble, prefibrillar oligomeric species [27]. As the oligomeric intermediates of the aggregation process exhibit extensive polymorphism, it is important for a molecule to generate non-toxic species before it can be considered for therapeutic applications [28].

In search of new agents that block the formation of disease associated protein aggregates we zeroed down on triphenylmethanes. It is one such group of unexploited molecules comprising oldest man-made dyes used extensively in industries as colouring agents for textiles, plastics etc. These dyes are basically hydrocarbons having skeletons of triphenyl methane. Some of these dyes such as Coomassie Brilliant Blue which were developed for the textile industry are now routinely used as biological stains for staining proteins in analytical biochemistry. Coomassie Brilliant Blue is the name of two similar triphenylmethane dyes Coomassie Brilliant Blue G-250 (CBBG) and Coomassie Brilliant Blue R-250 (CBBR) which differ from each other by two methyl groups. CBBG is a close analogue of Brilliant Blue FCF which is an FDA approved dye exploited extensively in food industries for imparting blue colour to food items. Both the dyes have excellent safety profile and are water soluble. Recently, CBBG was also reported to improve recovery in rat models of thoracic spinal cord injury [29]. It has also been shown useful for treatment of optic nerve injury [30]. Additionally, it crosses the BBB efficiently.

Taking all the significant characteristic features of the dyes into account, we hypothesized whether these dyes possessed effect against α-synuclein aggregation and toxicity. The fact that the first prerequisite of a molecule to act as an inhibitor of protein aggregation is its affinity for the protein also supported our proposition. In 2001, Lee et al. published a report studying the specific interaction of dyes with alpha-synuclein. They have underlined in their study that the dye interactions were independent from the acidic c-terminus and also separate from the Aβ 25–35 interaction site on alpha-synuclein. They have even suggested that these biologically specific interactions could be explored further for the development of diagnostic, preventive or therapeutic strategies [31]. As these dyes have ability to bind to proteins, we went on to investigate whether the dye binding to an aggregating α-synuclein proves beneficial.

In the present study, we have screened and compared the effect of two triphenylmethane dyes *viz.* Coomassie Brilliant Blue G (CBBG) and Coomassie Brilliant Blue R (CBBR) against α-synuclein aggregation, fibrillisation and modulation of neurotoxicity. With the help of several biochemical, biophysical, imaging and cell based assays we have shown for the first time that these dyes are potent aggregation inhibitors with varying toxicity modulation properties. Our study also emphasizes on the fact that arresting fibrillisation non-specifically is of no use till the production of cytotoxic species is altogether stopped or redirected to the production of non-toxic end products.

2. Materials and methods

2.1. Materials

RNase-DNase free water was purchased from Invitrogen-Gibco, USA. Ampicillin, ammonium acetate, ammonium sulphate, culture grade PBS, Luria broth, Luria Bertani agar, agarose, potassium choride, potassium hydroxide, calcium chloride, magnesium chloride, skimmed milk powder, streptomycin sulphate, sucrose and bovine serum albumin were from Himedia Labaratories Pvt. Ltd., India. Methanol, glacial acetic acid, dimethyl sulphoxide (DMSO), ethanol and hydrochloric acid were from Merck Lmt, India. DNA Marker, DNA 6X orange loading dye, unstained protein ladder and pre-stained protein marker were procured from Fermentas-Thermo Fischer Scientific, USA. Protease inhibitor tablets were from Roche, Switzerland. Uranyl acetate was bought from Polysciences Inc., Taiwan. Good View nucleic acid stain was from SBS Genetech, China. In Vitro Toxicology Assay Kit, Lactic Dehydrogenase based was from Sigma-Aldrich, CBBG and CBBR were from Sigma Aldrich and were marked as "pure". All other chemicals were from Sigma Aldrich USA, unless otherwise mentioned.

2.2. Methods

2.2.1. Preparation of ultra competent E. coli

A single bacterial colony of *E.Coli* competent cells were grown for 6–8 h in 25 mL Luria broth with vigorous shaking at 250–300 rpm. This culture was used to inoculate around three 250 mL cultures and was allowed to grow with moderate shaking at 18-22 °C for around 16 h. The OD_{600} was monitored every 45 min

till it reached 0.55 for any one flask. The other two flasks were then discarded. The flask with OD_{600} was kept in ice-water bath for 10 min. The cells were harvested by centrifugation at 2500 *g* for 10 min at 4 °C. The cells were then gently resuspended in 80 mL of INOUE buffer. Aliquots of 50 μL–100 μL were then made in pre-cooled microfuge tubes and stored at −80 °C for further use.

2.2.2. Transformation of plasmid in E. coli

Competent *E. coli* cells, stored at −80 °C and the plasmids were thawed on ice for about 20 min. 1–2 μL of the desired plasmid (about 100 ng) was added to about 50 μL of competent cells. The tubes were swirled gently several times to mix their contents and then incubated on ice for 30 min. Heat shock was given to the cells at 42 °C for 45–60 s and then rapidly transferred and incubated on ice for 5 min. The cells were then allowed to recover in 200 μL Luria Bertani (LB) medium at 37 °C with gentle shaking at 180 rpm in a shaker incubator, for 1 h. Transformed competent *E. coli* cells were plated onto LB agar plates containing the appropriate antibiotic and incubated by inverting the plates at 37 °C for 12 h.

2.2.3. Expression and purification of α-synuclein from pT7-7 clone

Both WT and A53T mutant α-synuclein protein were expressed from pT7-7 vector in BL21 *E. Coli* cells. Briefly, transformed cells induced with 1 mM IPTG were harvested 4 h post-induction by centrifugation at 5000 rpm for 15 min. Protein was purified by boiling the cell pellet resuspended in appropriate buffer followed by treatment with streptomycin sulphate (136 μL/ml), glacial acetic acid, saturated ammonium sulphate, 100 mM ammonium acetate and absolute ethanol as described in detail elsewhere [25]. MALDI and western blot with anti α-synuclein antibody were used to confirm the purity of protein. Inconsistencies caused due to batch variations were eliminated by pooling several preparations to get a single homogenous lot. Proteins, with measured concentrations using molecular weight 14.46 kDa and an extinction coefficient of 5960 $M^{-1}cm^{-1}$were aliquoted and stored at −20 °C.

2.2.4. Preparation of stock solution of triphenylmethane dyes

Stock solutions (1 mM) of the compounds were prepared in deionized water and final reaction mixtures contained equal amount of water.

2.2.5. Aggregation reaction

3 mg/mL (210 μM) of α-synuclein was allowed to undergo aggregation in 10 mM sodium phosphate buffer (pH 7.0) having 10 mM $MgCl_2$ and 0.05% sodium azide (aggregation buffer). A constant shaking at 180 rpm was given to the samples kept at 37 °C with or without equimolar concentration of compounds. Aliquots taken out at different time points were used for various biophysical assays.

2.2.6. Thioflavin T (ThT) assay

A stock solution of 5 mM Thioflavin T was prepared in deionized water and filtered through 0.2 μm polyether sulfone filter. 1 mL of 50 μM ThT prepared in Glycine-NaOH buffer, pH 8.0 was used as working solution to which 2 μL of 210 μM α-synuclein sample solution was diluted and incubated for 15 min at 25 °C in the dark. The resulting fluorescence intensities of ThT samples were measured using an excitation wavelength of 440 nm and 5 nm slit width at an emission wavelength of 480 nm using a Jobin Vyon Horiba Fluoromax-4 spectrofluorimeter. The corrected fluorescence was calculated using equation (1) which includes discrepancies due to inner filter effect.

$$Cf = Af \times anti\log[(Aex + Aem)/2] \quad (1)$$

Where Cf is the corrected fluorescence and Af is apparent fluorescence, Aex and Aem are the absorbances of the samples at excitation and emission wavelengths respectively. To account for differences in protein samples, all the measurements were normalized by subtracting the day 0 values from all the measured values. Percent change in fluorescence intensity and percent inhibition were calculated as described elsewhere [25].

Dose response curves were obtained using 3 parameter sigmoidal fitting and IC_{50} values were calculated from as shown in equation (2)

$$f = a/(1 + \exp(-(X - X0)/b)) \quad (2)$$

Where X is the log of concentration and X0 is the log of concentration at 50% inhibition.

2.2.7. Congo red assay

10 μL of protein samples were added to 190 μL of Congo Red (50 μM solution) and incubated for 1 h at 37 °C. Absorbance data were recorded after 1 h incubation on Shimadzu UV-VIS spectrophotometer as a spectrum from 400 to 600 nm.

2.2.8. Turbidity assay

To 145 μL of aggregation buffer 5 μL of protein samples were added and turbidity was measured by recording absorbance at 360 nm. The optical density (O.D) of a particular sample at the beginning of the experiment was subtracted from the final (O.D) to get change in turbidity.

2.2.9. Transmission electron microscopy (TEM)

3 μL of each aggregation sample was allowed to adsorb onto a Carbon coated Formvar mesh grid for 2 min followed by negative staining with 2% Uranyl acetate for 1 min. Transmission electron microscopy images were collected with a CM10 Philips operated at 80 kV after blotting dry the grids.

2.2.10. Atomic force microscopy (AFM)

All the aggregates were resuspended by mixing the samples gently. 5 μL of 50X diluted samples were adsorbed directly onto freshly cleaved mica, air dried followed with rinsing and a second round of drying under nitrogen flow. Imaging was done in non-contact acoustic AC mode using Atomic force microscope 5500(Agilent Technologies) and analyzed with SPIP software.

2.2.11. Dot-blot assay

3 μL of α-synuclein samples were spotted onto a nitrocellulose membrane dried at room temperature. Dot blotting was done using A11 antibody according to manufacturer's protocol [25]. The blot images were captured using a Digital imaging system –ImageQuant™ LAS 4000.

2.2.12. Cell culture

SH-SY5Y, the human neuroblastoma cell line was obtained from American Type Culture Collection (ATCC). Cells were grown at 37 °C in a humidified incubator with 5% CO_2 in Dulbecco's modified Eagle medium (DMEM, GIBCO) to which 10% fetal bovine serum (FBS, GIBCO) and 1 mM glutamine were added.

2.2.13. Determination of cytotoxicity by MTT assay

Colorimetric MTT [3-(4, 5-dimethyl-2-thiazolyl) - 2, 5-diphenyl-2Htetrazolium bromide] assay. SH-SY5Y cells were seeded at 5×10^4 cells/well in 96-well plates. After 12 h, the medium was

removed and replaced with media containing protein alone or with the tested compounds and left at 37 °C. After 24 h, spent medium was replaced with 90 μL of fresh medium and 10 μL of MTT (5 mg/mL) in PBS (0.5 mg/mL, final concentration). The cells were incubated for another 4 h. After the removal of MTT, formazan crystals formed were dissolved in acidified isopropanol. The amount of formazan was evaluated by measuring the optical density at 570 nm. Cell viability was expressed as the percentage of control cells and was calculated using the equation (3)

$$CV = (At/Au) \times 100 \quad (3)$$

Where CV is cell viability and At and Au are the absorbance of the treated and untreated neurons respectively after subtracting the absorbance of only MTT.

2.2.14. Determination of cytotoxicity by LDH assay

SH-SY5Y cells were seeded at 5×10^4 cells/well in 96-well plates. After 12 h, the medium was removed and replaced with media containing protein alone or with the tested compounds and left at 37 °C. The cells were again left for another 12 h s. The cultures were removed from incubator into a laminar flow hood and 1/10 volume of LDH Assay Lysis Solution was added per well and plate was returned to the incubator for 45 min. The plates were then centrifuged at 250 *g* for 4 min to pellet debris. Aliquots were transferred to clean flat-bottom plate and proceeded with enzymatic analysis. Equal volumes of LDH Assay Substrate, LDH Assay Dye Solution and LDH Assay Cofactor Preparation were mixed to prepare the Lactate Dehydrogenase Assay Mixture. This mixture was added in a volume double to the reaction mixture to be tested. The plate was covered with aluminium foil and incubated at room temperature for 20–30 min. Thereafter the reaction was terminated by the addition of 1/10 volume of 1 N HCl to each well. The absorbance was measured spectrophotometrically at a wavelength of 490 nm. The background absorbance of the multiwell plates at 690 nm was subtracted from the primary wavelength measurement (490 nm). The percentage viability in each sample was calculated by the following equation (4)

$$CV = (Rt/Ru) \times 100 \quad (4)$$

Where CV is the cell viability and Rt and Ru are the corrected absorbance of treated and untreated samples.

2.2.15. Optical microscopy

SH-SY5Y cells were grown up to around 60% confluence according to the protocol described for cell culture. SH-SY5Y cells were then co-incubated with 15 days aggregates of the WtAS (210 μM) alone and with equimolar concentration of the CBBG and CBBR under serum starvation condition for 12 h. Images were taken under the inverted light microscope (Nikon Eclipse TS100) at 40× magnification and analyzed using the software NIS-Elements F 4.00.00.

2.2.16. Statistical analyses

Results were expressed as the means and the standard deviation (S.D.) values, with n as the number of experiments. IC_{50} values were calculated from dose-dependency curves using Sigma Plot 10.0. P

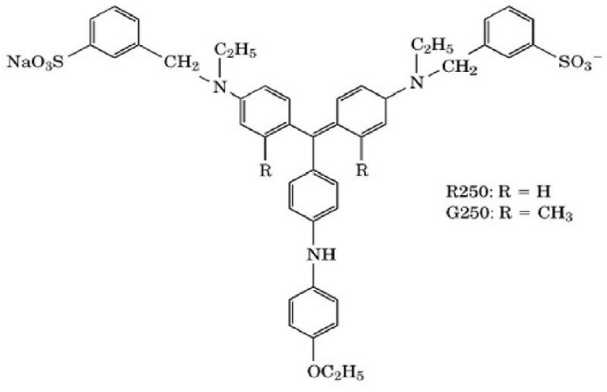

Fig. 1. Structure of Coomassie Brilliant Blue G250 (CBBG) and Coomassie Brilliant Blue R250 (CBBR). CBBG has two additional methyl groups.

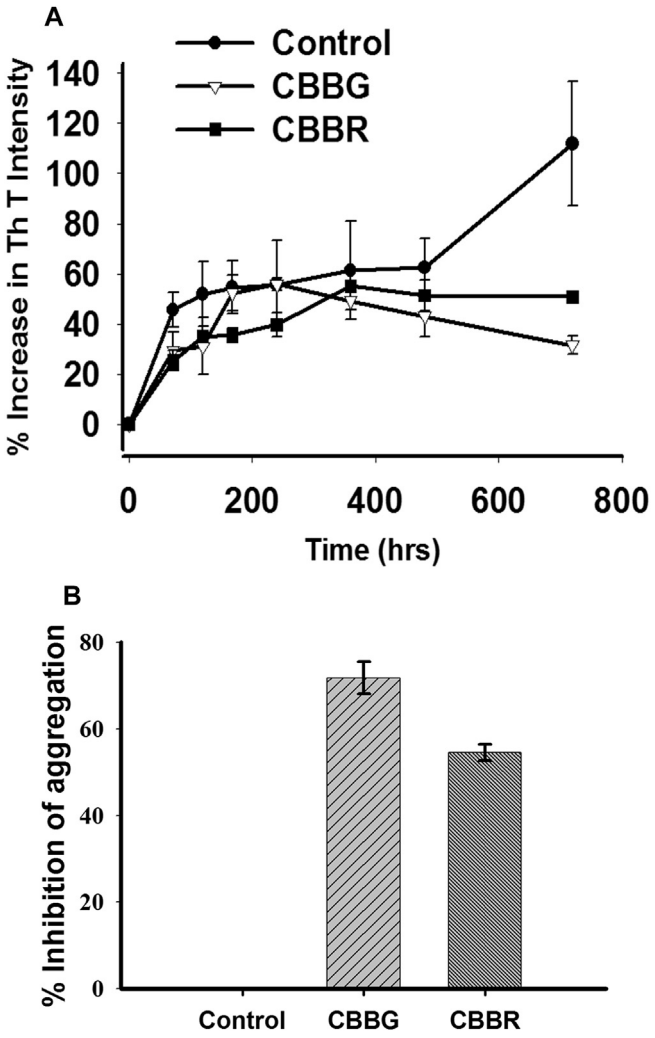

Fig. 2. A: Time course of WtAS aggregation in the presence or absence of compounds CBBG and CBBR as monitored by ThT assay. WtAS (210 μM) was co-incubated with equimolar concentration of CBBG and CBBR for 30 days. The ability of these dyes to prevent aggregation was monitored by ThT fluorescence. Aggregated samples were incubated with 50 μM of ThT for 30 min at 25 °C. Samples were excited at 440 nm and emissions recorded at 480 nm. Results are the mean of three different experiments done in duplicate and the error bars show the standard deviations.

B: Percentage inhibition of aggregation of WtAS by CBBG and CBBR as monitored by ThT assay. WtAS (210 μM) was co-incubated with equimolar concentration of CBBG and CBBR for 30 days. The ability of these dyes to prevent aggregation was monitored by ThT fluorescence. Aggregated samples were incubated with 50 μM of ThT for 30 min at 25 °C. Samples were excited at 440 nm and emissions recorded at 480 nm. Percent inhibition was calculated. Results are the mean of three different experiments done in duplicate and the error bars show the standard deviations. The p values for CCBG and CBBR were 0.03 and 0.04 respectively.

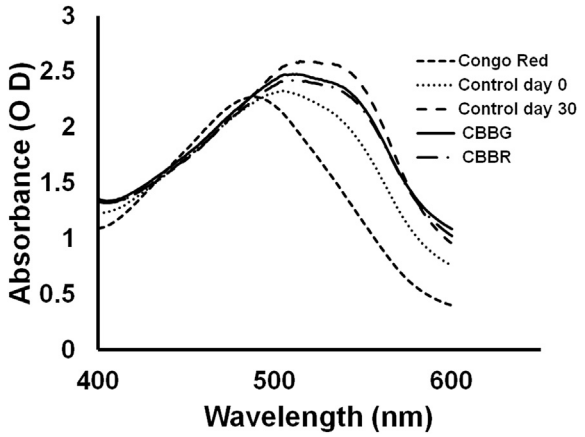

Fig. 3. Absorbance spectra of Congo Red of aggregated WtAS samples in the presence or absence of compounds CBBG and CBBR. WtAS (210 μM) was co-incubated with equimolar concentration of CBBG and CBBR for 30 days. The ability of these dyes to prevent aggregation was monitored by Congo red binding assay. Samples were incubated with 50 μM Congo Red for 1 h at 37 °C and Absorbance was scanned from 400 nm to 600 nm using UV–Vis spectrophotometer. Results are mean of three independent experiments done in duplicate.

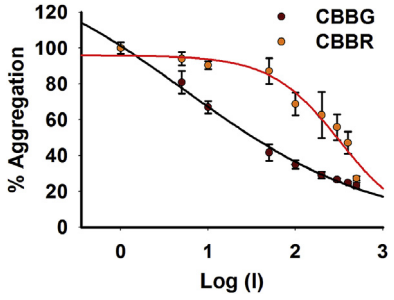

Fig. 4. Dose response curves for determination of IC_{50} values of CBBG and CBBR against WtAS aggregation. WtAS (210 μM) was co-incubated with various concentrations (1–500 μM) of **CBBG and CBBR** for 30 days. The ability of these dyes to prevent aggregation was monitored by ThT assay. Aggregated samples were incubated with 50 μM of ThT for 30 min at 25 °C. Samples were excited at 440 nm and emissions recorded at 480 nm. The percentage of aggregation was calculated by measuring corrected ThT fluorescence post 30 days of incubation and was plotted against log of compound concentration. The 3-parameter sigmoidal fit gives the best fit and IC_{50} values were calculated from the graph. Results are mean of three independent experiments done in duplicate and the error bars show the standard deviation.

values for significance were determined by unpaired Student's *t*-test. In all analyses, the null hypothesis was rejected at the 0.05 level.

3. Results and discussion

Wt and mutant α-synuclein ORF cloned in Plasmid pT7-7 was confirmed by sequencing. We used *E-coli* BL21 cells to express and purify α-synuclein and the purity of protein was validated by MALDI and Western blot (Fig-S1& S2- Supplementary information). We standardised the aggregation conditions and acquired TEM images of 30 days aggregated Wt and A53T mutant α-synuclein in 10 mM sodium phosphate buffer containing $MgCl_2$ (10 mM) - pH 7 at 37 °C and 180 rpm as shown in Fig-S3 (Supplementary information).

The structures of the compounds CBBG and CBBR as shown in Fig. 1 are similar except for the presence of two additional methyl groups in CBBG. Here, we have monitored triphenylmethane dyes CBBG and CBBR for their ability to prevent aggregation of α-synuclein. The results compare the activity of these two dyes relative to each other and WtAS alone.

3.1. Comparison of anti-amyloid activity of CBBG and CBBR and their effect on kinetics of WtAS fibrillisation and fibril morphology

We performed aggregation assay with α-synuclein alone as a control and in the presence of compounds CBBG and CBBR. Sampling was done at fixed intervals. To monitor the inhibitory effect of triphenylmethane dyes against WtAS fibrillation, we used Thioflavin T (ThT) assay. Thioflavin T is a benzo-thiazole dye that shows increase in fluorescence on binding to amyloid fibrils, especially the cross β-structures. ThT binding assay though employed widely as a screening method to study protein aggregation has a few limitations. Factors such as colour of the compounds and sample turbidity may quench ThT fluorescence, resulting in ThT bias and producing false positives [32]. We obviated all such probable inconsistencies by incorporating corrections for inner filter effect using equation (1). Moreover, ThT bias was further taken care of by calculating the percentage increase in fluorescence intensities rather than absolute intensities. Fig. 2A shows the kinetics of aggregation evidenced by an increase in fluorescence intensity of ThT. Our results showed clearly that both the compounds were effective in inhibiting α-synuclein aggregation. Percentage inhibition of aggregation calculated at the end of 30 day time period showed CBBG (71.8 ± 3 0.7) to be a more potent than CBBR (54.6 ± 1.9) (Fig. 2B). The data.

To further verify the inhibition of WtAS aggregation in the presence of CBBG and CBBR, we performed Congo Red binding assay. Congo red is a secondary diazo dye which binds to amyloid fibrils. Presence of cross β-sheet rich structures is indicated by the peak shift of Congo red absorption spectrum from 490 nm to 540 nm [33]. Fig. 3 clearly illustrates that co-incubation of WtAS with CBBG or CBBR prevented the red shift of peak of Congo red

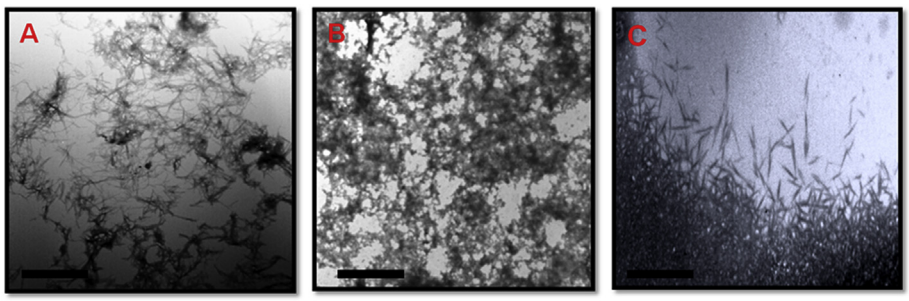

Fig. 5. Representative TEM images showing aggregate morphology of WtAS in the presence of CBBG and CBBR. WtAS (210 μM) was co-incubated with equimolar concentration of CBBG and CBBR for 30 days. The ability of these dyes to prevent aggregation was visualized by TEM. 3 μL aggregated samples were adsorbed on carbon coated formavar grids and negatively stained with 2% Uranyl acetate for TEM imaging. **(A)** WtAS (210 μM) alone at day 30 or in the presence of **(B)** CBBG **(C)** CBBR. Scale bar is 200 nm.

spectrum from 490 nm to 540 nm. Both ThT and Congo red data suggested that there was an obvious prevention of the formation of cross β-structures in WtAS protein samples in the presence of these triphenylmethane dyes.

For determining the difference in potencies of the dyes, IC50 values were measured. Briefly we incubated different concentrations of compounds CBBG and CBBR ranging from 1 μM to 500 μM with WtAS and monitored the ThT intensities. Percentage change in intensities were plotted against semi-log of compound concentrations using equation (2) for 3-parameter sigmoidal fitting as detailed elsewhere [34]. Dose-response curves (Fig. 4) were used to determine the inhibition potency of the dyes. 100% aggregationCalculations showed that while CBBR (322 ± 1.15 μM) inhibited WtAS at stoichiometric concentrations relative to WtAS, CBBG exhibited maximum effect with an IC_{50} value of 5.4 ± 1.99 μM. Compounds with extremely high activity and low IC50 values generate linear dose response curves rather than the usual sigmoidal curves as observed for CBBG [35].

In order to authenticate the results obtained through biophysical assays, we examined and characterized WtAS protein samples and those co-incubated with CBBG and CBBR using TEM and AFM imaging techniques.

As evidenced in Fig. 5A 30 day old WtAS fibrils were thin, long and formed clusters. Conversely, WtAS incubated with CBBG (Fig. 5B) or CBBR (Fig. 5C) did not attain fibrillar structure and were extremely different from each other. WtAS incubated with CBBG formed amorphous and globular aggregates whereas that incubated with CBBR exhibited mostly compact granular structures which were not mature fibrils. Since co-incubation with CBBG and CBBR yielded different structures from each other, it was presumed that these two dyes may have differences in their mode of action to prevent the fibril formation. Earlier in 2001, while studying the specific interaction of these dyes with alpha-synuclein, Lee et al. also clearly demonstrated that both the dyes have unique mode of

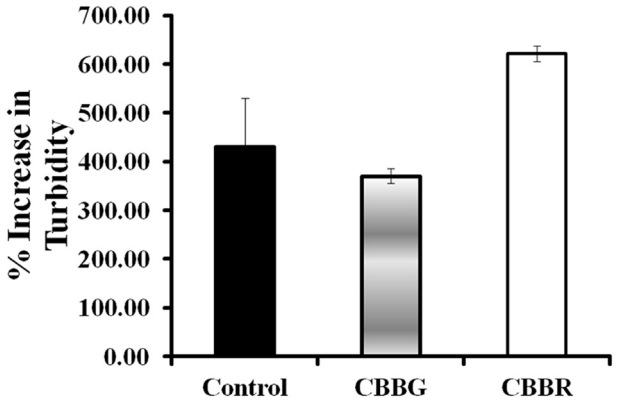

Fig. 7. Comparative bar diagram showing changes in turbidity of aggregated WtAS samples in the presence or absence of CBBG and CBBR. WtAS (210 μM) was co-incubated with equimolar concentration of CBBG and CBBR for 30 days. Subsequently, the turbidity of the samples was monitored. For this purpose 5 μL of WtAS aggregated samples were added to 145 μL of aggregation buffer and absorbance at 360 nm was recorded using UV–Vis spectrophotometer. Increase in turbidity was calculated by subtracting the turbidity at day 0. Results are mean of three independent experiments done in duplicate. P values are 0.3 and 0.03 for CBBG and CBBR respectively.

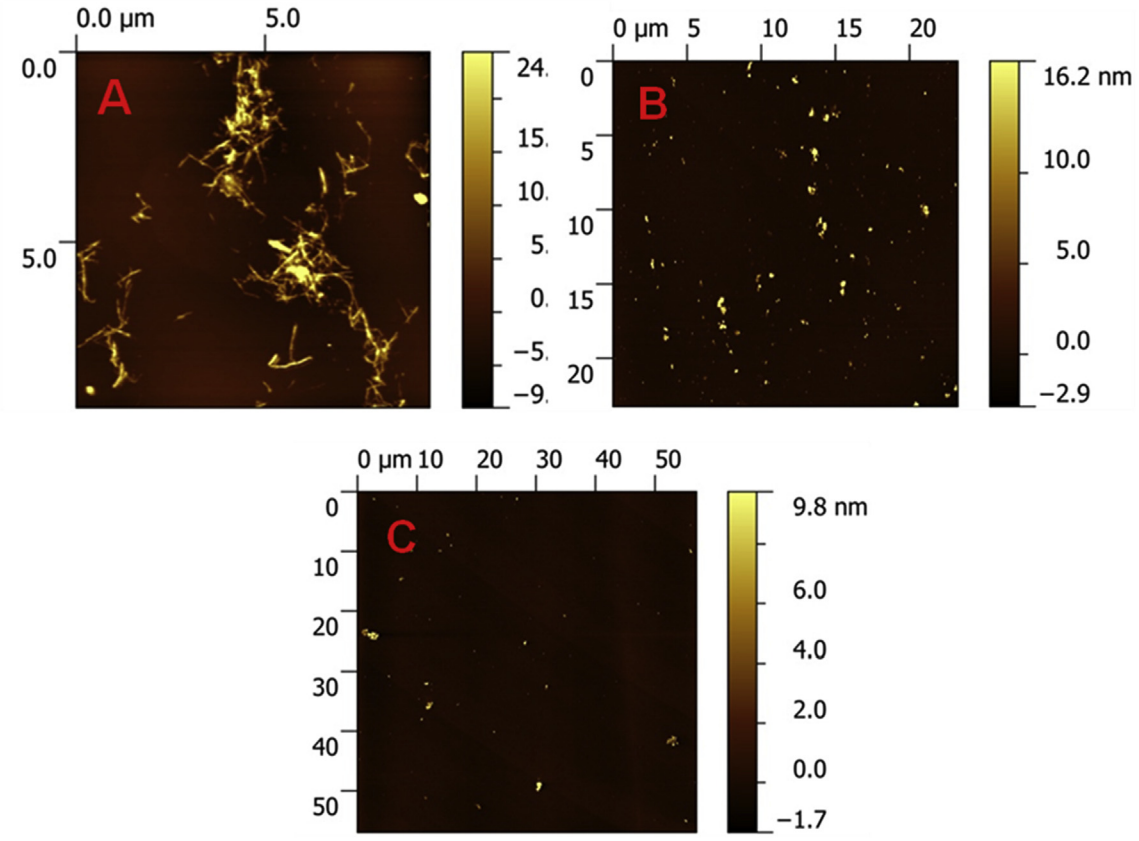

Fig. 6. Representative AFM images showing aggregate morphology of WtAS in the presence of CBBG and CBBR. WtAS (210 μM) was co-incubated with equimolar concentrations of CBBG and CBBR 30 days. The ability of these compounds to prevent aggregation was visualized by AFM. AFM topographic images of ultra structure of 50X diluted WtAS (210 μM) aggregates (**A**) alone at day 30 or in the presence of (**B**) CBBG (**C**) CBBR.

binding to the protein which results in different oligomer morphology.

Further the characterization of these end products of WtAS fibrillisation in the presence and absence of dyes were done using AFM. As illustrated in Fig. 6, control showed plenty of fully grown amyloid fibrils with heights of 1.9 ± 1.5 nm while products of protein aggregation in the presence of CBBG and CBBR imparted mostly oligomeric morphology. Yet, there were variations in the morphology, distribution and heights. Oligomers of WtAS generated in the presence of CBBG were comparatively larger (21.0 ± 2 nm) than in the presence of CBBR (6 ± 1 nm). The representative AFM image shown here for CBBR only shows oligomers as they were abundantly distributed in the sample studied. The compact fibrils were excluded from the picture shown.

Both TEM and AFM data, confirm the inhibitory activity of these two compounds as compared to control with a strong indication that in spite of the structural similarity of CBBG and CBBR, the minor dissimilarity in their structures may lead to different mode of action resulting in differences in the end species formed.

Time and again, it has been found that prefibrillar soluble oligomeric species are found to be more toxic and measurement of turbidity often gives an idea of the nature of aggregates formed depending on their solubility. Hence, we carried out turbidity measurements at 360 nm to understand the nature of oligomers

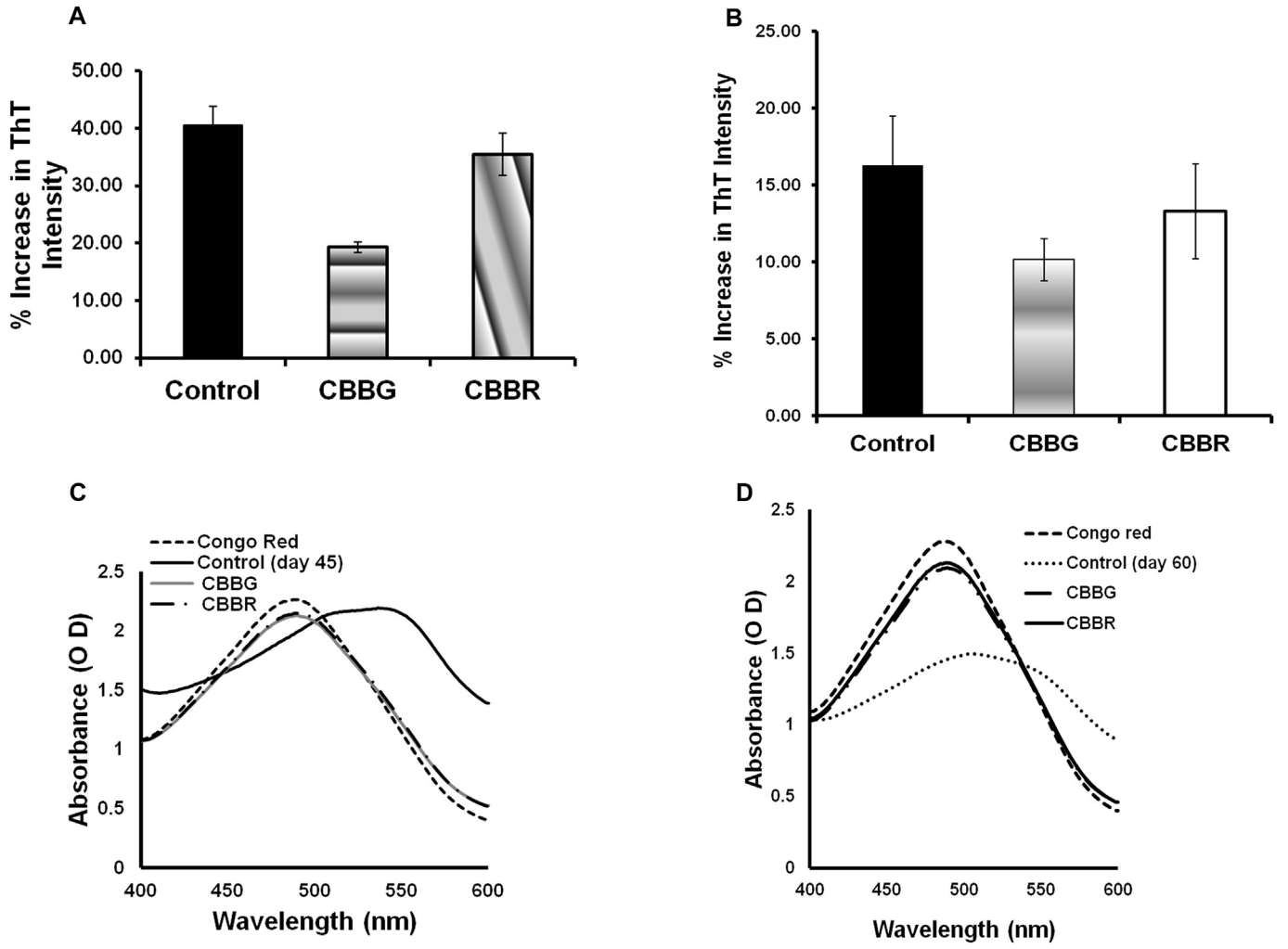

Fig. 8. A: **Comparative bar diagram showing the effect of CBBG and CBBR on 15 days aggregated WtAS by ThT assay**. WtAS (210 μM) samples were aggregated alone for 45 days or equimolar concentrations of CBBG and CBBR were added at day 15 and further co-incubated for 30 days. The ability of these dyes to prevent further aggregation was monitored by ThT assay. Aggregated samples were incubated with 50 μM of ThT for 30 min at 25 °C. The samples were excited at 440 nm and emissions recorded at 480 nm. Percentage increase in aggregation was calculated by measuring corrected ThT fluorescence intensity. Results are the mean of three different experiments done in duplicate and the error bars show the standard deviations. P values were 0.01 and 0.28 for CBBG and CBBR respectively.

B: **Comparative bar diagram showing the effect of CBBG and CBBR on 15 days aggregated WtAS by ThT assay**. WtAS (210 μM) samples were aggregated alone for 60 days or equimolar concentrations of CBBG and CBBR were added at day 30 and further co-incubated for 30 days. The ability of these dyes to prevent further aggregation was monitored by ThT assay. Aggregated samples were incubated with 50 μM of ThT for 30 min at 25 °C. The samples were excited at 440 nm and emissions recorded at 480 nm. Percentage increase in aggregation was calculated by measuring corrected ThT fluorescence intensity. P values for CBBG and CBBR were 0.14 and 0.28 respectively.

C: **Absorbance spectra of Congo Red of aggregated WtAS samples in the presence or absence of CBBG and CBBR on 15 days aggregated WtAS**. WtAS (210 μM) samples were aggregated alone for 45 days or equimolar concentrations of CBBG and CBBR were added at day 15 and further co-incubated for 30 days. The ability of these dyes to prevent further aggregation was monitored by Congo red binding assay. Samples were incubated with 50 μM Congo Red for 1 h at 37 °C and Absorbance was scanned from 400 nm to 600 nm using UV–Vis spectrophotometer. Results are mean of three independent experiments done in duplicate.

D: **Absorbance spectra of Congo Red of aggregated WtAS samples in the presence or absence of CBBG and CBBR on 30 days aggregated WtAS**. WtAS (210 μM) samples were aggregated alone for 60 days or equimolar concentrations of CBBG and CBBR were added at day 30 and further co-incubated for 30 days. The ability of these dyes to prevent further aggregation was monitored by Congo red binding assay. Samples were incubated with 50 μM Congo Red for 1 h at 37 °C and Absorbance was scanned from 400 nm to 600 nm using UV–Vis spectrophotometer. Results are mean of three independent experiments done in duplicate.

(Fig. 7). Percentage increase in turbidity was calculated and results showed that the increase in turbidity in the presence of WtAS samples was 430.9 ± 100.7. The increase in turbidity for CBBG on the other hand was 370.5 ± 100.7, almost half to that of CBBR (621.9 ± 15.8). Thus the results demonstrated that CBBR interaction resulted in the production of more insoluble aggregates as compared to CBBG or control.

3.2. Effect of triphenylmethane dyes on existing and pre-formed WtAS fibrils

Since the efficiency of an aggregation inhibitor is judged not only by its ability to prevent monomer association and conversion of oligomers into fibrils but also by disrupting pre-existing fibrils. We therefore tested whether CBBG and CBBR have the ability to overturn the aggregation process by halting the already ongoing process and disrupting the already existing fibrils. For this CBBG and CBBR were added to 15 days and 30 days preformed fibrils and incubation was extended for another 30 days. ThT and Congo red binding assays were then performed on day 45 (15 + 30) and day 60 (30 + 30) aggregates.

ThT assays done on day 45 samples showed that while WtAS registered a 40.4 ± 3.4% increase in fluorescence intensity after day 15, there was a significant decrease in ThT intensity for WtAS samples containing CBBG (19.3 ± 0.9) but not for CBBR (35.5 ± 3.7) (Fig. 8A). Assays done on day 60 samples showed only CBBG (10.2 ± 1.4) and not CBBR (13.3 ± 3.1) led to reduced fluorescence intensity as compared to WtAS control (16.3 ± 3.2) (Fig. 8B). The data indicated that while CBBG was effective in preventing elongation and disruption of existing fibrisl CBBR was marginally effective in this context.

Again Congo Red binding assays on day 45 (Fig. 8C) and day 60 (Fig. 8D) with WtAS samples containing CBBG and CBBR, showed a clear peak shift reversal. The results were in excellent agreement with ThT assay implying that both CBBG and CBBR were efficient in reducing the cross β-structures of preformed fibrils.

3.3. Effect of triphenylmethane dyes on WtAS oligomer toxicity

Interventional strategies concerning inhibition target largely the mature fibrils and the final fibril burden. However, arresting fibrillisation non-specifically is of limited value till the production of cytotoxic species is altogether stopped or redirected to production of non-toxic end products. A number of researchers have even considered the idea of accelerating the fibrillisation process, so as to convert the toxic oligomers into less harmful fibrils which may have its own drawbacks [36]. Whatever may be the case, determination of toxicity of the end species is crucial and modulation of toxicity is an essential feature for a molecule to be classified under therapeutic agents. Accumulating evidences suggest that it is the prefibrillar soluble oligomers which are harmful. A breakthrough was achieved in April 2003 when Kayed and group developed an antibody called A11 specifically against soluble pathogenic oligomers of all types [37].It recognised the oligomers irrespective of the protein species involved in oligomerisation.

Hence, to ascertain the toxicity we first carried out dot blot analysis with A11 antibody. Our results showed that WtAS aggregates alone exhibited maximum reactivity against A11 while CBBR successfully repressed the formation of this toxic epitope at the end of 30 days (Fig. 9). Surprisingly, presence of CBBG did not affect the appearance of A11 conformation in α-synuclein at all despite its reported ability to compromise the production of toxic Aβ oligomers [38]. The difference in behavior of CBBG and CBBR in modulating the toxicity of oligomeric intermediates of WtAS may be due to the presence of two additional methyl groups in CBBG that may have affected the binding of CBBG to α-synuclein. Such dissimilar interactions can either yield toxic species as in the case of CBBG or

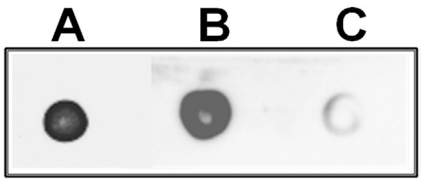

Fig. 9. Representative image of A11 antibody dot blot showing effect of CBBG and CBBR on WtAS A11 epitope formation. WtAS (210 μM) aggregated alone or co-incubated with equimolar concentration of CBBG and CBBR for 30 days. For dot blot analysis 3 μL of protein samples were spotted on a nitrocellulose membrane and probed with A11 antibody. **(A)** WtAS alone **(B)** CBBG **(C)** CBBR.

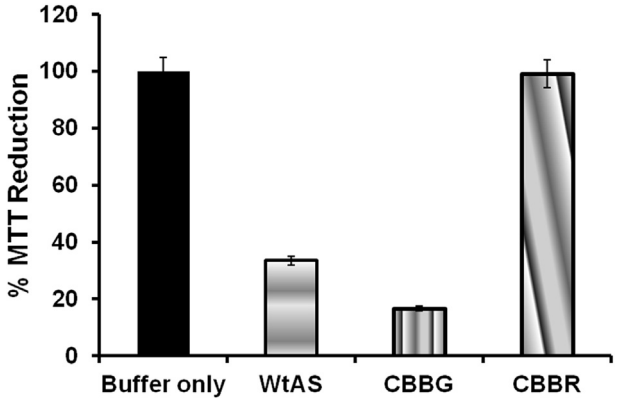

Fig. 10. Comparative bar diagram showing MTT reduction by oligomers of WtAS alone or co-incubated with CBBG and CBBR in neuronal culture. WtAS (210 μM) was aggregated alone or co-incubated with equimolar concentration of compounds CBBG and CBBR for 30 days. SH-SY5Y cells were co-incubated with 2 μL of above samples for 24 h followed by MTT addition. The products of MTT reduction were dissolved and colour was read at 570 nm. Percentage MTT reduction was calculated. Results are the mean of three different experiments done in duplicates and error bars show standard deviation.

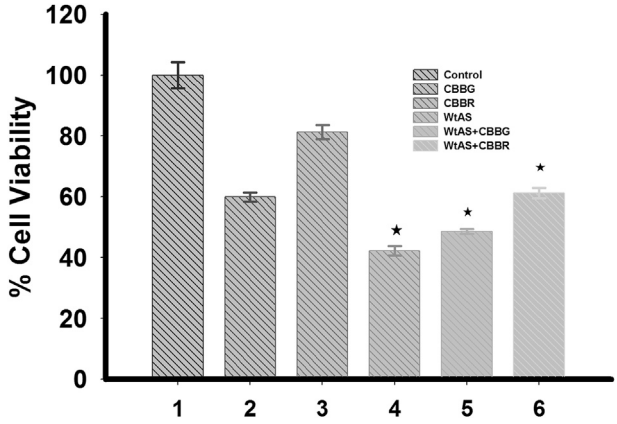

Fig. 11. Comparative bar diagram showing total LDH activity by oligomers of WtAS alone or co-incubated with CBBG and CBBR in neuronal culture. WtAS (210 μM) was aggregated alone or co-incubated with equimolar concentration of compounds CBBG and CBBR for 15 days. SH-SY5Y cells were co-incubated with 2 μL of above samples for 12 h followed by addition of LDH lysis solution and assay mixture as per protocol. The products of LDH activity were used to reduce a tetrazolium dye which was dissolved and the colour was read at 490 nm. Percentage cell viability was calculated. Results are the mean of three different experiments done in duplicates and error bars show standard deviation. P values for samples with CBBG and CBBR were 0.003 and 0.0003 respectively.

non-toxic intermediates seen in the case of CBBR.

In order to confirm the results obtained by A11 dot blot assays, the samples of aggregation assays with or without the addition of CBBG and CBBR were analyzed further by LDH and MTT assay. For this, we chose SH-SY5Y neuroblastoma cell line which is a neuronal adrenergic cell line used to study neuronal functions and is apt for studies related to PD as it expresses dopaminergic markers. Cell viability was measured using equation (3) and equation (4). The results of MTT assay showed that cells incubated with the protein samples containing CBBR resulted in around 99% MTT reduction and presented no toxic insults to neuronal cells. On the contrary, samples with CBBG resulted in profuse cell death, hence reduced only 19% of MTT and thus demonstrated extremely high neuronal toxicity (Fig. 10).

Furthermore the results of LDH assay which is a widely used method to measure cytotoxicity also showed higher neuronal toxicity for samples incubated with CBBG as compared to CBBR [39]. When total LDH activity was measured to calculate the cell viability, WtAS co-incubated with CBBR for 15 days showed 61% viable cells as compared to only 48% and 42% in samples containing CBBG and WtAS only respectively. In totality, LDH assay also demonstrated that CBBR was effective in alleviating the toxicity of WtAS oligomerisation (Fig. 11). Even images of cultures incubated with the 15 days aggregates in the presence or absence of compound corroborated with the results of A11, MTT and LDH assay. Cells with WtAS alone or with CBBG registered profuse cell death as opposed to the ones incubated with CBBR (Fig. 12).

Thus, the results of A11 immunoblot, MTT assay and LDH assay gave a clear indication that the oligomers of WtAS formed with incubation of CBBG were toxic.

3.4. Effect of triphenylmethane dyes on the inhibition of fibrillisation of the faster aggregating A53T mutant α-synuclein

As far as inhibition of α-synuclein aggregation is concerned, therapies should also be directed towards dealing with mutated forms of synuclein such as A53T and A30P mutations. Both these mutations are linked with early onset PD. The peculiarity of these mutations is an accelerated rate of oligomerisation compared to WT. Moreover, here again non-fibrillar oligomers play a crucial role

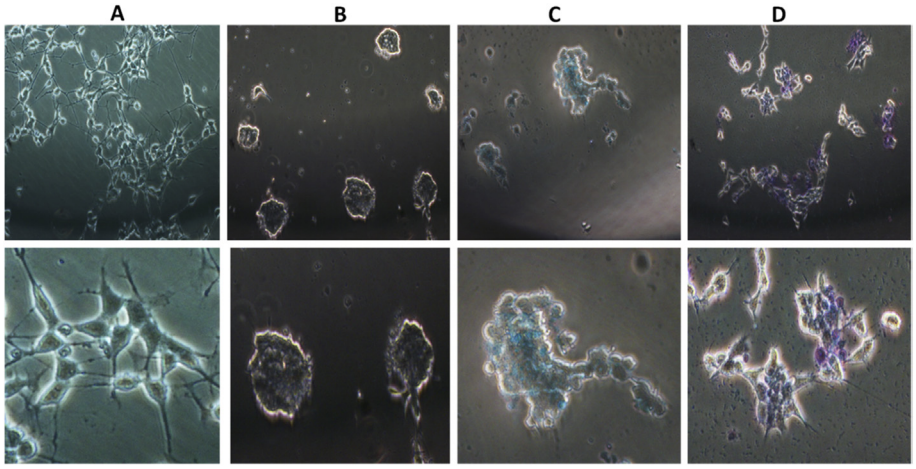

Fig. 12. Representative Optical microscopy images showing morphology of SH-SY5Y cells in the presence of WtAS with CBBG and CBBR. WtAS (210 μM) was co-incubated with equimolar concentration of CBBG and CBBR for 15 days. The aggregates thus obtained were incubated with SH-SY5Y cells for 12 h. Images were taken with inverted light microscope. Aggregation buffer served as control. SH-SY5Y cells with **(A)** Aggregation Buffer **(B)** WtAS (210 μM) alone at day 15 or in the presence of **(C)** CBBG **(D)** CBBR.

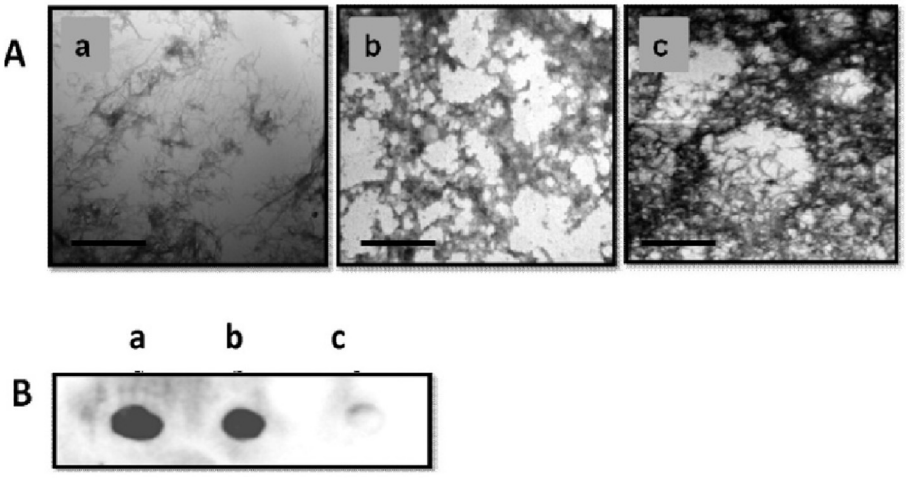

Fig. 13. Representative TEM micrographs and A11 dot blot images showing aggregate morphology and toxicity of A53T mutant α-synuclein alone or co-incubated with CBBG and CBBR. **A**. A53T mutant α-synuclein (210 μM) aggregated for 30 days **(a)** alone or in the presence of equimolar concentrations of **(b)** CBBG **(c)** CBBR. Scale bar is 200 nm. **B**. Representative image of A11 antibody dot blot showing effect of compounds CBBG and CBBR on A53T mutant α-synuclein A11 epitope formation. **(a)** WtAS alone **(b)** CBBG **(c)** CBBR.

in the pathogenesis [40].

Therefore, any effective therapy would entail dealing with toxicity issues of both WT and mutant synuclein.

As A53T mutant α-synuclein is more vigorously aggregating form of the protein and hence we wanted to test the efficacy of these compounds on the fibrillisation and toxicity modulation of A53T mutant form of the protein. Electron micrographs of TEM showed complete absence of any fibrillar structures and clear differences in morphology of aggregates in A53T mutant α-synuclein samples co-incubated with CBBG and CBBR (Fig. 13A). However, there was complete absence of any fibrillar structures in A53T α-synuclein incubated with these compounds. It was observed that CBBG co-incubation resulted in amorphous aggregates of A53T whilst CBBR caused formation of denser aggregates. In A11 dot blot assay, mutant α-synuclein samples incubated with CBBG showed A11 reactivity while CBBR showed very slight A11 reactivity. Hence, it was clear that CBBG failed to abolish the formation of toxic epitopes unlike CBBR which once again proved to be more efficient and potent modulator of toxicity as illustrated in Fig. 13B.

4. Conclusions

The outcome of the present study emphasizes the potential of CBBR as a small molecule inhibitor of α-synuclein aggregation and an efficient modulator of toxicity. While this work was in progress Wong et al. (2011) reported that triphenylmethanes have the ability to inhibit aggregation of Aβ peptide which provided impetus to our studies further [38]. In the present study, however, though both CBBG and CBBR displayed efficacy against α-synuclein aggregation and fibril formation, CBBG failed to prevent the formation of toxic species. The results once again highlight subtle differences in their therapeutic potential and a display of anti-amyloid activity nonetheless constitutes a first step towards finding a lead.

It is a common notion that different amyloidogenic proteins have similar mechanisms of aggregation and toxic aggregates have common epitopes as is evident by the fact that one antibody can recognise all of them [37]. Our study draws attention to the inherent complexities and differences of the misfolding and aggregation process in general. It underscores the idea that despite similarities, there are understated differences which rules out the existence of a panacea for all the aggregation related disorders. For example; CBBG does not modulate the toxic products of α-synuclein like it does for amyloid β [38].Similarly, Methylene blue has been shown to behave differently with different amyloidogenic protein. Reports suggest that it can modulate Aβ related toxicity but not tau and polyglutamine associated toxicities [41,42]. Hence, every molecule has to be studied individually in detail in relation to a particular protein to understand better, the mechanism of their aggregation and inhibition.

In conclusion, we report that CBBR may serve as a useful therapeutic molecule for α-synucleinopathies which can be taken one step ahead for further *in vivo* studies whereas CBBG though may not impart beneficial effects can still be used as a mechanistic tool for delineating the aggregation process and understanding the underlying intricacies of α-synuclein fibrillisation.

Acknowledgments

This work is supported by an extramural grant for Bhatnagar Fellowship to AS by the Council of Scientific and Industrial Research (CSIR), India and from the core grant of NII. NA is a SRF of DBT. The present work is also supported by NII Core and DBT grant (BT/PR12648/BRB/10/711/2009) to SG. Authors wish to thank Professor Rajiv Bhat, School of Biotechnology, Jawaharlal University, New Delhi for the gift of A53T mutant derived from the Wild type alpha synuclein by MKJ and Rajiv Bhat. Wild type alpha synuclein was a gift from Professor Peter Lansbury, Department of Neurology, Harvard Medical School, USA. Authors thank Mrs. Rekha Rani for technical assistance in acquiring TEM images.

Appendix A. Supplementary data

Supplementary data related to this article can be found at https://doi.org/10.1016/j.ejmech.2017.10.002.

References

[1] V.N. Uversky, Mysterious oligomerization of the amyloidogenic proteins, FEBS J. 277 (14) (2010) 2940–2953.
[2] L. Breydo, J.W. Wu, V.N. Uversky, Alpha-synuclein misfolding and Parkinson's disease, Biochim. Biophys. Acta 1822 (2) (2012) 261–285.
[3] V.N. Uversky, H.J. Lee, J. Li, A.L. Fink, S.J. Lee, Stabilization of partially folded conformation during alpha-synuclein oligomerization in both purified and cytosolic preparations, J. Biol. Chem. 276 (47) (2001) 43495–43498.
[4] J.M. Souza, B.I. Giasson, Q. Chen, V.M. Lee, H. Ischiropoulos, Dityrosine cross-linking promotes formation of stable alpha -synuclein polymers. Implication of nitrative and oxidative stress in the pathogenesis of neurodegenerative synucleinopathies, J. Biol. Chem. 275 (24) (2000) 18344–18349.
[5] M.J. Marti, E. Tolosa, J. Campdelacreu, Clinical overview of the synucleinopathies, Mov. Disord. 18 (Suppl 6) (2003) S21–S27.
[6] H. Shimura, M.G. Schlossmacher, N. Hattori, M.P. Frosch, A. Trockenbacher, R. Schneider, Y. Mizuno, K.S. Kosik, D.J. Selkoe, Ubiquitination of a new form of alpha-synuclein by parkin from human brain: implications for Parkinson's disease, Science 293 (5528) (2001) 263–269.
[7] T. Bartels, J.G. Choi, D.J. Selkoe, alpha-Synuclein occurs physiologically as a helically folded tetramer that resists aggregation, Nature 477 (7362) (2011) 107–110.
[8] W. Wang, I. Perovic, J. Chittuluru, A. Kaganovich, L.T. Nguyen, J. Liao, J.R. Auclair, D. Johnson, A. Landeru, A.K. Simorellis, S. Ju, M.R. Cookson, F.J. Asturias, J.N. Agar, B.N. Webb, C. Kang, D. Ringe, G.A. Petsko, T.C. Pochapsky, Q.Q. Hoang, A soluble alpha-synuclein construct forms a dynamic tetramer, Proc. Natl. Acad. Sci. U. S. A. 108 (43) (2011) 17797–17802.
[9] M. Hashimoto, M. Yoshimoto, A. Sisk, L.J. Hsu, M. Sundsmo, A. Kittel, T. Saitoh, A. Miller, E. Masliah, NACP, a synaptic protein involved in Alzheimer's disease, is differentially regulated during megakaryocyte differentiation, Biochem. Biophys. Res. Commun. 237 (3) (1997) 611–616.
[10] W. Tamo, T. Imaizumi, K. Tanji, H. Yoshida, F. Mori, M. Yoshimoto, H. Takahashi, I. Fukuda, K. Wakabayashi, K. Satoh, Expression of alpha-synuclein, the precursor of non-amyloid beta component of Alzheimer's disease amyloid, in human cerebral blood vessels, Neurosci. Lett. 326 (1) (2002) 5–8.
[11] U. Dettmer, A.J. Newman, V.E. von Saucken, T. Bartels, D. Selkoe, KTKEGV repeat motifs are key mediators of normal alpha-synuclein tetramerization: their mutation causes excess monomers and neurotoxicity, Proc. Natl. Acad. Sci. U. S. A. 112 (31) (2015) 9596–9601.
[12] C.B. Lucking, A. Brice, Alpha-synuclein and Parkinson's disease, Cell Mol. Life Sci. 57 (13–14) (2000) 1894–1908.
[13] P.H. Weinreb, W. Zhen, A.W. Poon, K.A. Conway, P.T. Lansbury Jr., NACP, a protein implicated in Alzheimer's disease and learning, is natively unfolded, Biochemistry 35 (43) (1996) 13709–13715.
[14] O. Marques, T.F. Outeiro, Alpha-synuclein: from secretion to dysfunction and death, Cell Death Dis. 3 (2012) e350.
[15] P.T. Lansbury, H.A. Lashuel, A century-old debate on protein aggregation and neurodegeneration enters the clinic, Nature 443 (7113) (2006) 774–779.
[16] T. Hard, C. Lendel, Inhibition of amyloid formation, J. Mol. Biol. 421 (4–5) (2012) 441–465.
[17] H. Zhang, L.Q. Xu, S. Perrett, Studying the effects of chaperones on amyloid fibril formation, Methods 53 (3) (2011) 285–294.
[18] R. Pul, R. Dodel, M. Stangel, Antibody-based therapy in Alzheimer's disease, Expert Opin. Biol. Ther. 11 (3) (2011) 343–357.
[19] S.I. Yoo, M. Yang, J.R. Brender, V. Subramanian, K. Sun, N.E. Joo, S.H. Jeong, A. Ramamoorthy, N.A. Kotov, Inhibition of amyloid peptide fibrillation by inorganic nanoparticles: functional similarities with proteins, Angew. Chem. Int. Ed. Engl. 50 (22) (2011) 5110–5115.
[20] C. Cabaleiro-Lago, F. Quinlan-Pluck, I. Lynch, S. Lindman, A.M. Minogue, E. Thulin, D.M. Walsh, K.A. Dawson, S. Linse, Inhibition of amyloid beta protein fibrillation by polymeric nanoparticles, J. Am. Chem. Soc. 130 (46) (2008) 15437–15443.
[21] Y. Porat, A. Abramowitz, E. Gazit, Inhibition of amyloid fibril formation by polyphenols: structural similarity and aromatic interactions as a common inhibition mechanism, Chem. Biol. Drug Des. 67 (1) (2006) 27–37.
[22] A. Abelein, L. Lang, C. Lendel, A. Graslund, J. Danielsson, Transient small molecule interactions kinetically modulate amyloid beta peptide self-assembly, FEBS Lett. 586 (22) (2012) 3991–3995.
[23] D.E. Ehrnhoefer, J. Bieschke, A. Boeddrich, M. Herbst, L. Masino, R. Lurz, S. Engemann, A. Pastore, E.E. Wanker, EGCG redirects amyloidogenic

polypeptides into unstructured, off-pathway oligomers, Nat. Struct. Mol. Biol. 15 (6) (2008) 558–566.
[24] M. Necula, R. Kayed, S. Milton, C.G. Glabe, Small molecule inhibitors of aggregation indicate that amyloid beta oligomerization and fibrillization pathways are independent and distinct, J. Biol. Chem. 282 (14) (2007) 10311–10324.
[25] N. Ahsan, S. Mishra, M.K. Jain, A. Surolia, S. Gupta, Curcumin Pyrazole and its derivative (N-(3-Nitrophenylpyrazole)) Curcumin inhibit aggregation, disrupt fibrils and modulate toxicity of Wild type and Mutant alpha-Synuclein, Sci. Rep. 5 (9862) (2015).
[26] F. Yang, G.P. Lim, A.N. Begum, O.J. Ubeda, M.R. Simmons, S.S. Ambegaokar, P.P. Chen, R. Kayed, C.G. Glabe, S.A. Frautschy, G.M. Cole, Curcumin inhibits formation of amyloid beta oligomers and fibrils, binds plaques, and reduces amyloid in vivo, J. Biol. Chem. 280 (7) (2005) 5892–5901.
[27] C.G. Glabe, Structural classification of toxic amyloid oligomers, J. Biol. Chem. 283 (44) (2008) 29639–29643.
[28] M. Fandrich, Oligomeric intermediates in amyloid formation: structure determination and mechanisms of toxicity, J. Mol. Biol. 421 (4–5) (2012) 427–440.
[29] W. Peng, M.L. Cotrina, X. Han, H. Yu, L. Bekar, L. Blum, T. Takano, G.F. Tian, S.A. Goldman, M. Nedergaard, Systemic administration of an antagonist of the ATP-sensitive receptor P2X7 improves recovery after spinal cord injury, Proc. Natl. Acad. Sci. U. S. A. 106 (30) (2009) 12489–12493.
[30] M. Ridderstrom, M. Ohlsson, Brilliant blue G treatment facilitates regeneration after optic nerve injury in the adult rat, Neuroreport 25 (17) (2014) 1405–1410.
[31] D. Lee, E.K. Lee, J.H. Lee, C.S. Chang, S.R. Paik, Self-oligomerization and protein aggregation of alpha-synuclein in the presence of Coomassie Brilliant Blue, Eur. J. Biochem. 268 (2) (2001) 295–301.
[32] S.A. Hudson, H. Ecroyd, T.W. Kee, J.A. Carver, The thioflavin T fluorescence assay for amyloid fibril detection can be biased by the presence of exogenous compounds, FEBS J. 276 (20) (2009) 5960–5972.
[33] W.E. Klunk, R.F. Jacob, R.P. Mason, Quantifying amyloid by Congo red spectral shift assay, Methods Enzymol. 309 (1999) 285–305.
[34] N. Ahsan, S. Mishra, M.K. Jain, A. Surolia, S. Gupta, Curcumin Pyrazole and its derivative (N-(3-Nitrophenylpyrazole)) Curcumin inhibit aggregation, disrupt fibrils and modulate toxicity of Wild type and Mutant α-Synuclein, Sci. Rep. 5 (2015).
[35] M. Caruana, T. Hogen, J. Levin, A. Hillmer, A. Giese, N. Vassallo, Inhibition and disaggregation of alpha-synuclein oligomers by natural polyphenolic compounds, FEBS Lett. 585 (8) (2011) 1113–1120.
[36] P.K. Singh, V. Kotia, D. Ghosh, G.M. Mohite, A. Kumar, S.K. Maji, Curcumin modulates alpha-synuclein aggregation and toxicity, ACS Chem. Neurosci. 4 (3) (2013) 393–407.
[37] R. Kayed, E. Head, J.L. Thompson, T.M. McIntire, S.C. Milton, C.W. Cotman, C.G. Glabe, Common structure of soluble amyloid oligomers implies common mechanism of pathogenesis, Science 300 (5618) (2003) 486–489.
[38] H.E. Wong, W. Qi, H.M. Choi, E.J. Fernandez, I. Kwon, A safe, blood-brain barrier permeable triphenylmethane dye inhibits amyloid-beta neurotoxicity by generating nontoxic aggregates, ACS Chem. Neurosci. 2 (11) (2011) 645–657.
[39] G. Fotakis, J.A. Timbrell, In vitro cytotoxicity assays: comparison of LDH, neutral red, MTT and protein assay in hepatoma cell lines following exposure to cadmium chloride, Toxicol. Lett. 160 (2) (2006) 171–177.
[40] K.A. Conway, S.J. Lee, J.C. Rochet, T.T. Ding, R.E. Williamson, P.T. Lansbury, Jr., Acceleration of oligomerization, not fibrillization, is a shared property of both alpha-synuclein mutations linked to early-onset Parkinson's disease: implications for pathogenesis and therapy, Proc. Natl. Acad. Sci. U. S. A. 97 (2) (2000) 571–576.
[41] D.X. Medina, A. Caccamo, S. Oddo, Methylene blue reduces abeta levels and rescues early cognitive deficit by increasing proteasome activity, Brain Pathol. 21 (2) (2011) 140–149.
[42] F. van Bebber, D. Paquet, A. Hruscha, B. Schmid, C. Haass, Methylene blue fails to inhibit Tau and polyglutamine protein dependent toxicity in zebrafish, Neurobiol. Dis. 39 (3) (2010) 265–271.